NJC

Accepted Manuscript

This is an *Accepted Manuscript*, which has been through the Royal Society of Chemistry peer review process and has been accepted for publication.

Accepted Manuscripts are published online shortly after acceptance, before technical editing, formatting and proof reading. Using this free service, authors can make their results available to the community, in citable form, before we publish the edited article. We will replace this *Accepted Manuscript* with the edited and formatted *Advance Article* as soon as it is available.

You can find more information about *Accepted Manuscripts* in the Information for Authors.

Please note that technical editing may introduce minor changes to the text and/or graphics, which may alter content. The journal's standard Terms & Conditions and the Ethical guidelines still apply. In no event shall the Royal Society of Chemistry be held responsible for any errors or omissions in this *Accepted Manuscript* or any consequences arising from the use of any information it contains.

ROYAL SOCIETY OF CHEMISTRY

www.rsc.org/njc

From Spiropentane to Butterfly and Tetrahedral Structures in Tetranuclear Iron Carbonyl Carbide Chemistry

Xiaoli Gong,*[a] Liyao Zhu,[a] Jing Yang,[b] Xiumin Gao,[a] Qian-shu Li,[c] Yaoming Xie,[d] R. Bruce King,*[c,d] and Henry F. Schaefer III[d]

[a]*College of Electronic Information, Hangzhou Dianzi University, Hangzhou 310018, China*

[b]*Department of Chemistry, Tangshan Normal College, Tangshan 063000, P. R China*

[c]*MOE Key Laboratory of Theoretical Environmental Chemistry, Center for Computational Quantum Chemistry, South China Normal University, Guangzhou 510631, China*

[d]*Department of Chemistry and Center for Computational Quantum Chemistry, University of Georgia, Athens, Georgia 30602, USA*

e-mails: rbking@chem.uga.edu and gxl@hdu.edu.cn

Abstract

Oxidative degradation of the octahedral dianion $[Fe_6C(CO)_{16}]^{2-}$ with an interstitial carbon atom leads eventually to the neutral $Fe_4C(CO)_{13}$ cluster with a butterfly-shaped central Fe_4C unit. The complete series of related $Fe_4C(CO)_n$ (n = 16, 15, 14, 13, 12, 11) derivatives have now been investigated using density functional theory. For the lowest energy $Fe_4C(CO)_n$ (n = 16, 15, 14, 13) structures the geometries obey the $n + f = 18$ rule where f is the number of Fe–Fe bonds. This leads to a spiropentane geometry with two Fe–Fe bonds for $Fe_4C(CO)_{16}$, a central bent Fe–Fe–Fe–Fe chain for $Fe_4C(CO)_{15}$, a distorted trigonal pyramidal structure with four Fe–Fe bonds for $Fe_4C(CO)_{14}$, and the experimentally observed butterfly structure with five Fe–Fe bonds for $Fe_4C(CO)_{13}$. A symmetrical higher energy centered tetrahedral structure for $Fe_4C(CO)_{12}$ with six Fe–Fe bonds also follows the $n + f = 18$ rule. However, the lowest energy $Fe_4C(CO)_n$ (n = 12, 11) structures are derived from the lowest energy $Fe_4C(CO)_{13}$ structure by removal of CO groups with retention of the central Fe_4C butterfly unit.

1. Introduction

The chemistry of metal carbonyl carbide clusters originated with the 1962 discovery of the iron carbonyl carbide $Fe_5C(CO)_{15}$ cluster as an unexpected stable side product isolated in trace quantities (<0.5%) after careful chromatographic separation from mixtures obtained from certain reactions of iron carbonyls with alkynes.[1] The structure of $Fe_5C(CO)_{15}$ was shown by X-ray diffraction to consist of an Fe_5 square pyramid partially enclosing an interstitial carbon atom bonded to all five iron atoms (Figure 1).

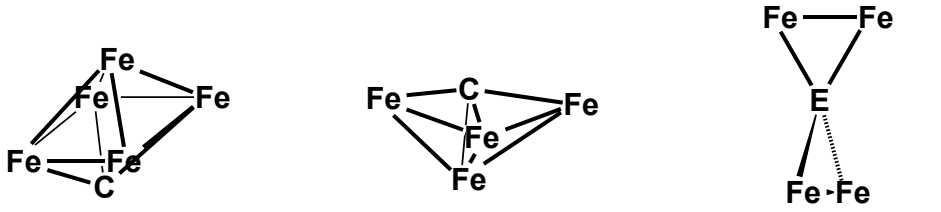

Figure 1. The cluster frameworks for the known species $Fe_5C(CO)_{15}$, $Fe_4C(CO)_{13}$, and $E[Fe_2(CO)_8]_2$ (E = Si, Ge, Sn, Pb). Carbonyl groups are omitted for clarity.

The very low yield (<1%) in the original synthesis of $Fe_5C(CO)_{15}$ initially discouraged the development of the chemistry of iron carbonyl carbide clusters. Eventually, however, synthetic methods were developed providing more reasonable yields of $Fe_5C(CO)_{15}$ as well as other iron carbonyl carbide and related clusters. A key was the discovery of the reaction of $Fe(CO)_5$ with the metal carbonyl anions $Mn(CO)_5^-$ or $V(CO)_6^-$ in boiling diglyme[2,3] to give reasonable yields of the hexanuclear octahedral iron carbonyl carbide dianion $[C@Fe_6(CO)_{16}]^{2-}$ having an interstitial carbon atom at the center of an Fe_6 octahedron. This octahedral iron carbonyl cluster proved to be a useful source of smaller iron carbonyl carbide clusters by partial degradation. Thus acidification of this dianion with H_2SO_4 provides an improved method for the synthesis of $Fe_5C(CO)_{15}$. In addition, oxidative degradation of $[C@Fe_6(CO)_{16}]^{2-}$ in methanol using reagents such as tropylium bromide leads to the tetranuclear $[Fe_4C(CO)_{12}(CO_2CH_3)]^-$ anion.[4] Acidification of this anion with trifluoromethanesulfonic acid gives the neutral tetranuclear iron carbonyl carbide $Fe_4C(CO)_{13}$.[5] X-ray crystallography indicates a butterfly structure for $Fe_4C(CO)_{13}$ with a CFe_2 triangle forming the body of the butterfly and the remaining two iron atoms the wingtips (Figure 1). Such iron carbonyl carbide clusters have subsequently proven to be useful precursors for the synthesis of larger mixed metal

carbonyl carbide clusters.[6,7,8] In addition, these iron carbonyl carbide clusters have been the subject of spectroscopic and theoretical studies. Thus in 1982, Sosinsky et al.[9] reported a study of the spectra of a series of iron carbide clusters, including $[Fe_4C(CO)_{12}]^{2-}$. Two years later, independent theoretical studies by Hoffmann et al.[10] and Harris et al.[11] discussed the bonding, electron counting, and reactivity of this these iron carbonyl carbide clusters. In 1987, vibrational frequencies of $[Fe_4C(CO)_{12}]^{2-}$ was measured by Stanghellini et al.[12] In 1988 Shriver reviewed the interaction of carbonyl monoxide with metal carbonyl carbide clusters including Fe_4C species.[13]

The structures of these iron carbonyl carbides, including the neutral species $Fe_4C(CO)_{13}$ and $Fe_5C(CO)_{15}$ as well as the centered octahedral dianion $[C@Fe_6(CO)_{16}]^{2-}$, can be rationalized using the Wade-Mingos rules,[14,15,16,17] which historically were developed to understand the structures of polyhedral boranes. For $Fe_4C(CO)_{13}$ and $Fe_5C(CO)_{15}$, in which the carbon atom is not completely surrounded by iron atoms, alternative models can be considered with the carbon atom considered either as a vertex atom or as an interstitial atom. In either case the carbon atom contributes all four of its valence electrons to the skeletal bonding. Both $Fe_4C(CO)_{13}$ and $Fe_5C(CO)_{15}$ are seen to be 14 skeletal electron systems, isolobal in the broad sense with the known boranes B_4H_{10} and B_5H_9, respectively. The central Fe_5C and Fe_4C skeletons of these species can be derived from the $C@Fe_6$ skeleton of the $[C@Fe_6(CO)_{16}]^{2-}$ precursor for their syntheses by removal of a single iron vertex and two adjacent iron vertices, respectively.

Analogous iron carbonyl clusters containing interstitial atoms of the heavier analogues of carbon, namely the tetrels Si, Ge, Sn, and Pb, remain unknown. However, carbonyl-richer tetranuclear iron carbonyl complexes of the tetrels of stoichiometries $EFe_4(CO)_{16}$ are stable species that have been synthesized by a variety of methods. The silicon[18] and lead[19] species have been shown by X-ray crystallography to have spiropentane-like structures (Figure 1) with a distorted tetrahedral coordination of the central tetrel atom to the four iron atoms. The four iron atoms are joined pairwise by iron-iron bonds so these structures may be more accurately described as $E[Fe_2(CO)_8]_2$. A carbon analogue of these spiropentane-like species, namely $C[Fe_2(CO)_8]_2$, has not been reported. Similar analogues of the iron carbonyl carbide clusters mentioned above with the heavier tetrel atoms, namely $Fe_4E(CO)_{13}$ and $Fe_5E(CO)_{15}$ (E = Si, Ge, Sn, Pb), remain unknown.

In summary there are two types of stable tetranuclear iron carbonyl derivatives $Fe_4E(CO)_n$ of the tetrels (C, Si, Ge, Sn, Pb). The stable carbon derivative is $Fe_4C(CO)_{13}$ with 13 carbonyl groups and a central Fe_4 butterfly structure with five formal Fe–Fe single bonds. However, the stable derivatives of the heavier tetrels are $Fe_4E(CO)_{16}$ (E =

Si, Ge, Sn, Pb) have spiropentane-like structures with 16 carbonyl groups and only two Fe–Fe single bonds. Thus the stable carbon derivative $Fe_4C(CO)_{13}$ has three fewer CO groups than the stable derivatives $E[Fe_2(CO)_8]_2$ of its heavier congeners. In order to gain some insight concerning these systems we have now investigated the entire series of tetranuclear iron carbonyl derivatives $CFe_4(CO)_n$ (n = 16, 15, 14, 13, 12, 11) with carbon as the central tetrel atom.

2. Theoretical Methods

Electron correlation effects were considered by employing density functional theory (DFT), which has evolved as a practical and effective computational tool, especially for organometallic compounds.[20,21,22,23,24,25,26] Two DFT methods were used in this study, namely the B3LYP and BP86 methods. The popular B3LYP method combines the three-parameter Becke exchange functional (B3)[27] with the Lee-Yang-Parr generalized gradient correlation functional (LYP).[28] The BP86 method combines Becke's 1988 exchange functional (B)[29] with Perdew's 1986 gradient corrected correlation functional (P86).[30] In general, these two methods predict geometries and relative energies in reasonable agreement. However, the BP86 method has been found to predict vibrational frequencies closer to experimental results.[31,32]

For consistency with our previous research, double-ζ plus polarization (DZP) basis sets were adopted in the present study. Thus, one set of pure spherical harmonic d functions with orbital exponents $\alpha_d(C) = 0.75$ and $\alpha_d(O) = 0.85$ for carbon and oxygen, respectively, was added to the standard Huzinaga-Dunning contracted DZ sets,[33,34] designated as (9s5p1d/4s2p1d). The loosely contracted DZP basis set for iron is the Wachters primitive set[35] augmented by two sets of p functions and one set of d functions, contracted following Hood, Pitzer and Schaefer,[36] designated as (14s11p6d/10s8p3d).

The geometries of all structures were fully optimized using the two DFT methods. Harmonic vibrational frequencies and the corresponding infrared intensities were evaluated analytically. All computations were performed with the Gaussian 03 program package.[37] The fine grid (75, 302) was the default for evaluating integrals numerically. All of the predicted triplet structures in the present study are found to have negligible spin contamination, with the S(S+1) values close to the ideal outcome of 2.0. The energies reported in the text and figures are those obtained after zero point vibrational correction.

A given $Fe_4C(CO)_n$ structure is designated as **nA-c** where **n** is the number of CO groups, **c** orders the structures according to their relative energies, and **A** indicates whether the structure is a singlet (**S**) or triplet (**T**). Thus the lowest energy singlet structure of $Fe_4C(CO)_{16}$ is designated **16S-1**.

3. Results and Discussion

3.1. $Fe_4C(CO)_n$ (n = 16 to 11) structures

The Fe_4C skeletons in the $Fe_4C(CO)_n$ compounds (n = 16 to 11) studied in the present paper are of four different types, namely spiropentane, triangular pyramidal, butterfly, and tetrahedral (Figure 2). Each skeletal type has four Fe-C bonds but different numbers of Fe-Fe bonds. The spiropentane skeleton generally has only two Fe-Fe bonds. However, in some cases the spiropentane skeleton is distorted so that an iron atom in each Fe_2C triangle can form a third Fe-Fe bond. The triangular skeleton normally has three Fe-Fe bonds but may have four Fe-Fe bonds if the Fe_3 base is distorted to place an additional pair of iron atoms within bonding distance. The butterfly and tetrahedral skeletons normally have five and six Fe-Fe bonds, respectively.

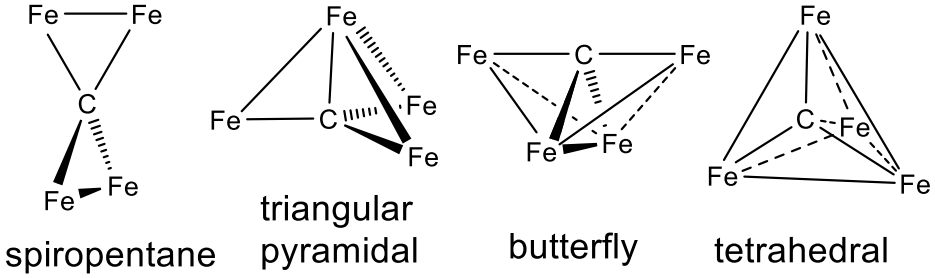

Figure 2. The fundamental Fe_4C skeletons in the $Fe_4C(CO)_n$ (n = 16 to 11) compounds.

3.1.1 $Fe_4C(CO)_{16}$. Three singlet structures were found for $Fe_4C(CO)_{16}$ within 20 kcal/mol of the global minimum (Figure 3 and Table 1). Structures **16S-1** and **16S-2** are predicted to be genuine minima with all real vibrational frequencies. The B3LYP and the BP86 methods differ in the relative energy ordering of these structures. The B3LYP method predicts **16S-1** to lie 3.4 kcal/mol in energy (with zero-point vibrational energy correction) below **16S-2**. However, the BP86 method predicts **16S-2** to lie 2.3 kcal/mol in energy below **16S-1**. Since these energy differences are small, these two structures may be considered to be nearly degenerate in energy. The third $Fe_4C(CO)_{16}$ structure **16S-3** is a higher energy structure, lying 17.2 kcal/mol (B3LYP) or 4.3 kcal/mol (BP86) in energy above **16S-1**.

The D_{2d} spiropentane structure **16S-1** has exclusively terminal CO groups (Figure 3 and Table 1). The two symmetry equivalent Fe–Fe distances in **16S-1** of 2.654 Å (B3LYP) or 2.637 Å (BP86) correspond to formal single bonds, thereby giving each iron atom the favored 18-electron configuration. The C_{2v} spiropentane structure **16S-2** has two

bridging CO groups connecting the Fe3 and Fe4 atoms (the lower two Fe atoms in Figure 3), but only terminal CO groups on the Fe1 and Fe2 atoms (the upper two Fe atoms in Figure 3). The bridging CO groups exhibit ν(CO) frequencies at 1859 and 1879 cm^{-1}, which are ~90 cm^{-1} below the lowest terminal ν(CO) frequency in accord with expectation.

Table 1. The carbon-iron bond distances (in Å) and the iron-iron bond distances (in Å) for the three $Fe_4C(CO)_{16}$ structures obtained by the B3LYP and BP86 methods.

	B3LYP			BP86		
	16S-1	**16S-2**	**16S-3**	**16S-1**	**16S-2**	**16S-3**
C_1-Fe_1	2.123	2.094	2.133	2.110	2.081	2.117
C_1-Fe_2	2.123	2.094	2.133	2.110	2.081	2.117
C_1-Fe_3	2.123	2.151	2.133	2.110	2.138	2.117
C_1-Fe_4	2.123	2.151	2.133	2.110	2.138	2.117
Fe_1-Fe_2	2.654	2.632	2.517	2.637	2.619	2.509
Fe_3-Fe_4	2.654	2.511	2.517	2.637	2.504	2.509

In **16S-2** the unbridged Fe1–Fe2 distance is 2.632 Å (B3LYP) or 2.619 Å (BP86) but the doubly bridged Fe3–Fe4 distance is significantly shorter by ~0.1 Å at 2.511 Å (B3LYP) or 2.504 Å (BP86). Both Fe-Fe distances can correspond to the formal single bonds required to give each iron atom the favored 18-electron configuration.

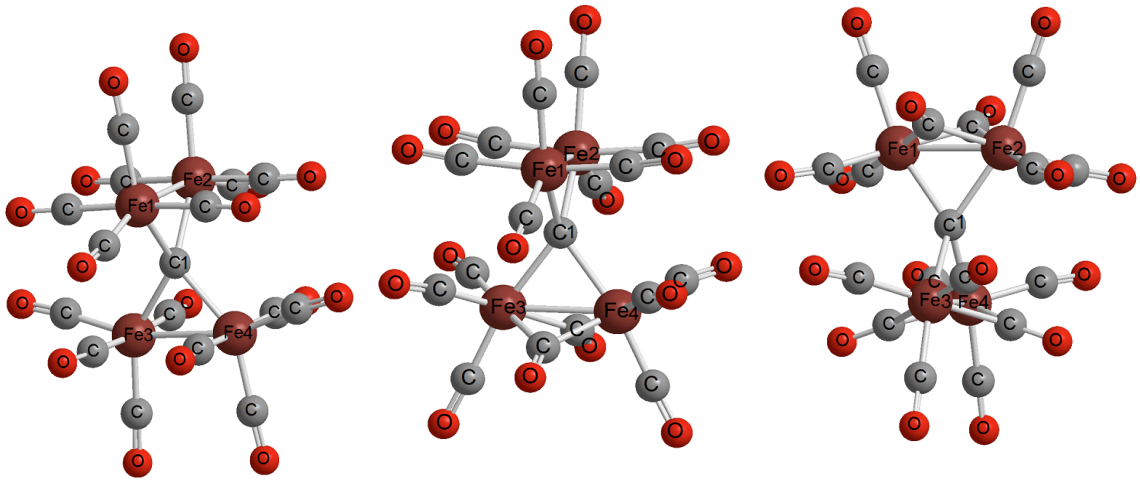

16S-1 (D_{2d}, 0.0, 0.0) **16S-2** (C_{2v}, 3.4, –2.3) **16S-3** (D_{2d}, 17.2, 4.3)

Figure 3. Three optimized singlet $Fe_4C(CO)_{16}$ structures.

The $Fe_4C(CO)_{16}$ structure **16S-3** of D_{2d} symmetry has a pair of CO groups bridging each of the two Fe-Fe bonds. The two symmetry equivalent doubly bridged Fe–Fe distances in **16S-3** of 2.517 Å (B3LYP) or 2.509 Å (BP86) correspond to formal single bonds, thereby giving each iron atom the favored 18-electron configuration. The doubly bridged Fe–Fe single bonds in **16S-3** are significantly shorter than the unbridged Fe–Fe single bonds in **16S-1**. Both DFT methods predict **16S-3** to have three small imaginary frequencies of 28*i*, 17*i*, and 17*i* cm^{-1} (B3LYP) or 25*i*, 18*i*, and 18*i* cm^{-1} (BP86). Following the corresponding normal mode leads to **16S-1**.

3.1.2 $Fe_4C(CO)_{15}$. The B3LYP and BP86 methods both predict structure **15S-1** to have a distorted spiropentane Fe_4C skeleton (Figure 4 and Table 2). The Fe1-Fe2 and Fe3-Fe4 distances of ~2.65 Å (B3LYP) or ~2.49 Å (BP86) suggest formal Fe-Fe single bonds. However, in contrast to the $Fe_4C(CO)_{16}$ structures, the Fe_4C skeleton in **15S-1** is distorted so that an additional pair of iron atoms (Fe1–Fe3) is within bonding distance, albeit a longer distance of 2.811 Å (B3LYP) or 2.691 Å (BP86). Thus, the four iron atoms in **15S-1** form a bent Fe_4 chain so that there are three Fe–Fe single bonds in the Fe_4C skeleton of **15S-1**, thereby giving each iron atom the favored 18-electron configuration assuming that the Fe1–Fe3 bond in the C_1 structure is polarized. The B3LYP method predicts a C_1 structure for **15S-1** with all fifteen CO groups in **15S-1** as terminal CO groups. However, the BP86 method predicts **15S-1** to have five bridging CO groups with C_2 symmetry. This accounts for the significantly shorter Fe–Fe distances in **15S-1** by the BP86 method relative to the B3LYP method.

Table 2. The carbon-iron bond distances (in Å) and the iron-iron bond distances (in Å) for the two $Fe_4C(CO)_{15}$ structures obtained by the B3LYP and BP86 methods.

	B3LYP		BP86	
	15S-1	**15S-2**	**15S-1**	**15S-2**
C_1-Fe_1	1.833	1.918	1.960	1.913
C_1-Fe_2	2.108	2.054	2.008	2.043
C_1-Fe_3	2.193	1.678	1.960	1.689
C_1-Fe_4	2.013	---	2.008	---
Fe_1-Fe_2	2.629	2.748	2.491	2.725
Fe_2-Fe_3	---	2.981	---	2.991
Fe_3-Fe_4	2.678	2.750	2.491	2.694
Fe_1-Fe_3	2.811	---	2.691	---

The $Fe_4C(CO)_{15}$ structure **15S-2**, lying 1.8 kcal/mol (B3LYP) or 8.3 kcal/mol (BP86) above **15S-1**, is a C_1 singlet structure with one bridging CO group (Figure 4). In contrast to the Fe_4C skeletons illustrated in Figure 2, the carbide carbon atom is bonded to only three iron atoms, leading to a linear arrangement of the Fe1-C-Fe3-Fe4 atoms combined with Fe2 to give a bent chain of four iron atoms. The bridging CO group in **15S-2** exhibits a ν(CO) frequency at 1820 cm^{-1}, which is ~130 cm^{-1} below the lowest terminal ν(CO) frequency in accord with expectation.

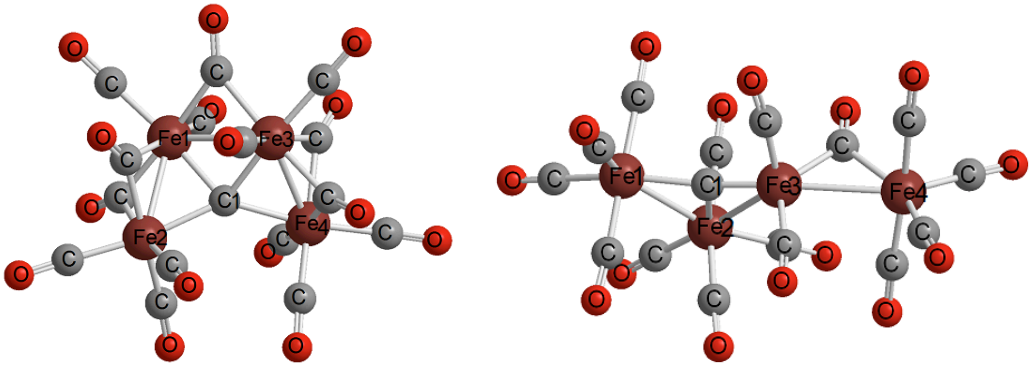

15S-1 (C_2/C_1, 0.0, 0.0) **15S-2** (C_1, 1.8, 8.3)

Figure 4. Two optimized singlet $Fe_4C(CO)_{15}$ structures.

3.1.3 $Fe_4C(CO)_{14}$. One low-lying singlet structure **14S-1** and one low-lying triplet structure **14T-1** for $Fe_4C(CO)_{14}$ are depicted in Figure 5. Other $Fe_4C(CO)_{14}$ structures with significantly higher relative energies are listed in the Supporting Information. The C_1 singlet structure **14S-1** has a distorted triangular pyramidal central Fe_4C unit with three unbridged Fe–Fe bonds (~2.7 Å) and one short bridged Fe–Fe bond of 2.590 Å (B3LYP) or 2.546 Å (BP86) (Table 3). These four Fe–Fe distances correspond to formal single bonds, thereby giving each iron atom the favored 18-electron configuration.

The C_1 triplet $Fe_4C(CO)_{14}$ structure **14T-1**, lying 4.7 kcal/mol (B3LYP) or 15.9 kcal/mol (BP86) above **14S-1**, has one bridging CO group (Figure 5). The four iron atoms in **14T-1** form a bent chain so that there are only three Fe–Fe bonds, each of which can be interpreted as a formal single bond. This gives two of the four iron atoms in **14T-1** the favored 18-electron configuration but the other two iron atoms only 17-electron configurations consistent with the triplet spin state. In **14T-1** the bridged Fe–Fe bonding distance of 2.510 Å (B3LYP) or 2.499 Å (BP86) is significantly shorter than the unbridged Fe–Fe bonding distances of 2.620 and 2.709 Å (B3LYP) or 2.559 and 2.670 Å (BP86) in accord with expectation.

Table 3. The carbon-iron bond distances and the iron-iron bond distances for the two $Fe_4C(CO)_{14}$ structures obtained by the B3LYP and BP86 methods.

	B3LYP		BP86	
	14S-1	**14T-1**	**14S-1**	**14T-1**
C_1-Fe_1	1.873	1.914	1.897	1.952
C_1-Fe_2	1.864	2.009	1.905	1.959
C_1-Fe_3	2.050	1.978	1.972	1.961
C_1-Fe_4	1.990	1.998	1.973	1.995
Fe_1-Fe_2	2.590	2.510	2.546	2.499
Fe_1-Fe_3	2.703	2.709	2.687	2.670
Fe_2-Fe_3	2.746	---	2.694	---
Fe_3-Fe_4	2.687	2.620	2.684	2.559

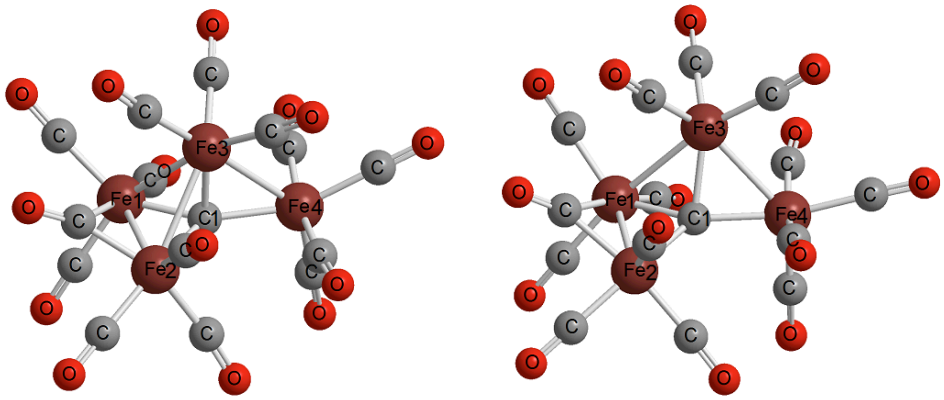

14S-1 (C_1, 0.0, 0.0) **14T-1** (C_1, 4.7, 15.9)

Figure 5. One optimized singlet $Fe_4C(CO)_{14}$ structure and one optimized triplet $Fe_4C(CO)_{14}$ structure.

3.1.4 $Fe_4C(CO)_{13}$.

For $Fe_4C(CO)_{13}$ several singlet structures and one triplet structure were optimized. The two lowest energy structures **13S-1** and **13T-1** are depicted in Figure 6, whereas the remaining higher energy structures are listed in the Supporting Information. Structure **13S-1** is a C_{2v} singlet structure with one bridging CO group (connecting Fe3 and Fe4 in Figure 6). This structure corresponds to the experimentally observed $Fe_4C(CO)_{13}$ structure characterized by X-ray crystallography.[5] The Fe_4C skeleton in **13S-1** no longer

has a spiropentane configuration, but a butterfly configuration in agreement with experimental observation. The Fe-C distances in the linear Fe-C-Fe subunit involving the butterfly wingtips (Fe1 and Fe2 in Figure 6) are predicted to be 1.802 Å (B3LYP) or 1.812 Å (BP86), which are close to the averaged experimental value of 1.789 Å (Table 4). The other two Fe-C distances in the Fe_4C skeleton (involving Fe3 and Fe4 in Figure 6) are predicted to be 2.008 Å (B3LYP) or 2.000 Å (BP86), which are also in excellent agreement with the averaged experimental value of 1.993 Å. The four equivalent predicted Fe–Fe distances of 2.663 Å (B3LYP) or 2.651 Å (BP86) in **13S-1** agree well with the averaged experimental values of 2.642 Å. The remaining Fe–Fe distance of 2.609 Å (B3LYP) or 2.568 Å (BP86) corresponding to the body of the butterfly agrees with the experimental value of 2.545 Å. The presence of five Fe–Fe single bonds in the butterfly structure **13S-1** gives each iron atom the favored 18-electron configuration.

Table 4. The predicted carbon-iron bond distances and the iron-iron bond distances for the two $Fe_4C(CO)_{13}$ structures obtained by the B3LYP and BP86 methods and the experimental distances obtained by X-ray crystallography.

	B3LYP		BP86		Exp[5]
	13S-1	**13T-1**	**13S-1**	**13T-1**	
C_1-Fe_1	1.802	1.798	1.812	1.824	1.799
C_1-Fe_2	1.802	1.922	1.812	1.904	1.779
C_1-Fe_3	2.008	1.926	2.000	1.925	1.998
C_1-Fe_4	2.008	1.907	2.000	1.882	1.987
Fe_1-Fe_2	---	2.750	---	2.711	---
Fe_2-Fe_3	2.663	2.606	2.651	2.579	2.637
Fe_1-Fe_3	2.663	2.665	2.651	2.629	2.642
Fe_1-Fe_4	2.663	---	2.651	---	2.647
Fe_2-Fe_4	2.663	---	2.651	---	2.640
Fe_3-Fe_4	2.609	2.621	2.568	2.600	2.545

The $Fe_4C(CO)_{13}$ structure **13S-1** is obviously a very favorable structure since the next lowest energy structure, namely the C_1 doubly bridged triplet structure **13T-1**, lies 15.5 kcal/mol (B3LYP) or 20.5 kcal/mol (BP86) above **13S-1** (Figure 6). The bridging CO groups in **13T-1** are predicted to exhibit ν(CO) frequencies at 1862 and 1879 cm^{-1}. The Fe_4C skeleton in **13T-1** is an irregular triangular pyramid with four Fe–Fe bonds and the C atom in the center of the base similar to the Fe_4C skeleton in the $Fe_4C(CO)_{14}$ structure **14S-1**. The two bridged Fe–Fe bonds are 2.606 and 2.621 Å (B3LYP) or 2.579

and 2.600 Å (BP86), whereas the unbridged Fe-Fe bonds are only slightly longer at 2.665 and 2.750 Å (B3LYP) or 2.629 and 2.711 Å (BP86). The presence of four Fe–Fe single bonds in **13T-1** gives two of the iron atoms (Fe2 and Fe3 in Figure 6) the favored 18-electron configuration but the other two iron atoms (Fe1 and Fe4 in Figure 6) only a 17 electron configuration consistent with the triplet spin state.

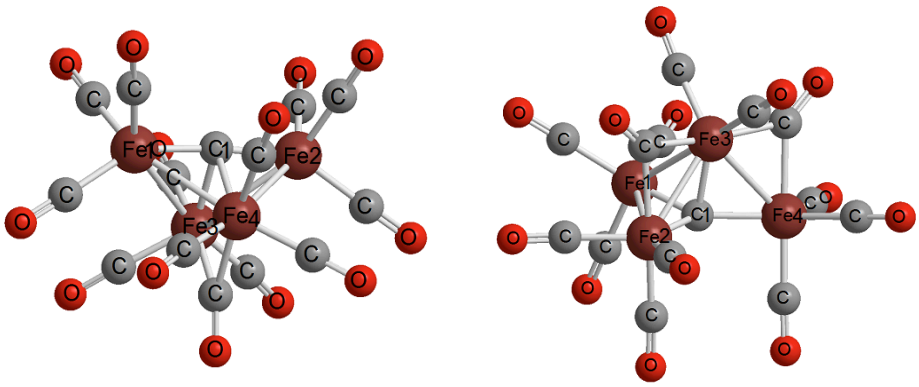

13S-1 (C_{2v}, 0.0, 0.0) **13T-1** (C_1, 15.5, 20.5)

Figure 6. Optimized $Fe_4C(CO)_{13}$ structures. The experimental bond distances[5] (averaged) for **13S-1** are listed under the DFT predicted results for comparison.

3.1.5 $Fe_4C(CO)_{12}$.

Three low-lying structures for $Fe_4C(CO)_{12}$ (two singlets and one triplet) were found within 20 kcal/mol (Figure 7 and Table 5). All three structures **12S-1, 12S-2**, and **12T-1** have exclusively terminal CO groups and are predicted to be genuine minima with all real vibrational frequencies.

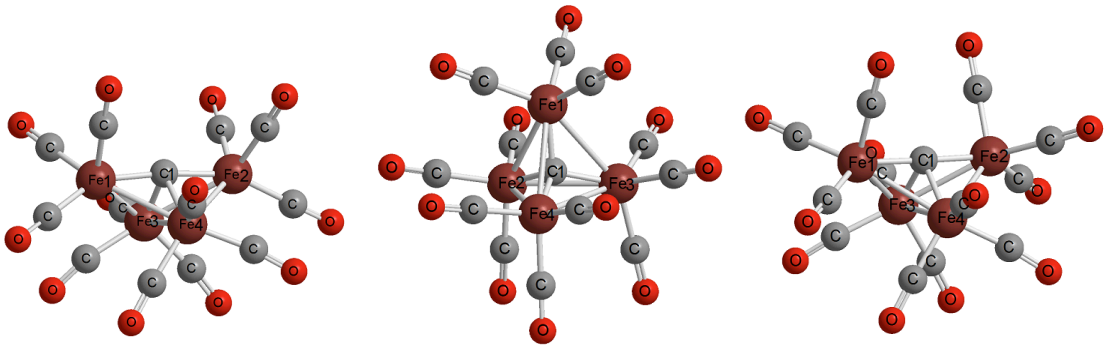

12S-1 (C_1, 0.0, 0.0) **12S-2** (T_d, 12.1, 16.8) **12T-1** (C_1, 1.8, 9.4)

Figure 7. Three optimized $Fe_4C(CO)_{12}$ structures.

The global minimum $Fe_4C(CO)_{12}$ structure **12S-1** is a C_1 singlet structure with a butterfly-shaped Fe_4C skeleton containing five Fe–Fe bonds (Figure 7). The Fe-C distances in the linear Fe-C-Fe subunit involving the butterfly wingtips (Fe1 and Fe2 in Figure 7) are predicted to be 1.834 Å and 1.846 Å (B3LYP) or 1.846 Å and 1.866 Å (BP86). The other two Fe-C distances in the Fe_4C skeleton (involving Fe3 and Fe4 in Figure 7) are predicted to be 1.899 Å and 1.892 Å (B3LYP) or 1.874 Å and 1.875 Å (BP86). The four Fe–Fe distances involving a wingtip iron atom are predicted to be 2.560, 2.645, 2.623, and 2.563 Å (B3LYP) or 2.527, 2.636, 2.583, and 2.547 Å (BP86) in **12S-1**. The remaining Fe–Fe distance predicted to be 2.858 Å (B3LYP) or 2.764 Å (BP86) corresponds to the body of the butterfly. The presence of five Fe–Fe single bonds in the butterfly structure **12S-1** gives each iron atom the favored 18-electron configuration. Structure **12S-1** can be derived from **13S-1** by removal of the bridging CO group.

Table 5. The carbon-iron bond distances and the iron-iron bond distances for the three $Fe_4C(CO)_{12}$ structures obtained by the B3LYP and BP86 methods.

	B3LYP			BP86		
	12S-1	**12S-2**	**12T-1**	**12S-1**	**12S-2**	**12T-1**
C_1-Fe_1	1.834	1.765	1.840	1.846	1.772	1.835
C_1-Fe_2	1.846	1.765	1.837	1.866	1.772	1.835
C_1-Fe_3	1.899	1.765	1.837	1.874	1.772	1.862
C_1-Fe_4	1.892	1.765	1.835	1.875	1.772	1.862
Fe_1-Fe_2	---	2.883	---	---	2.894	---
Fe_1-Fe_3	2.560	2.883	2.705	2.527	2.894	2.587
Fe_1-Fe_4	2.645	2.883	2.628	2.636	2.894	2.660
Fe_2-Fe_3	2.623	2.883	2.654	2.583	2.894	2.660
Fe_2-Fe_4	2.563	2.883	2.668	2.547	2.894	2.587
Fe_3-Fe_4	2.858	2.883	2.764	2.764	2.894	2.673

The C_1 triplet $Fe_4C(CO)_{12}$ structure **12T-1**, lying 1.8 kcal/mol (B3LYP) or 9.4 kcal/mol (BP86) above **12S-1**, has a geometry similar to **12S-1** (Figure 7). The beautifully symmetrical T_d singlet $Fe_4C(CO)_{12}$ structure **12S-2**, lying 11.2 kcal/mol (B3LYP) or 15.9 kcal/mol (BP86) above **12S-1**, has a tetrahedral Fe_4C skeleton, similar to the geometry of isoelectronic $Co_4(CO)_{12}$.[38] The isolated carbon atom is located inside the Fe_4 tetrahedron. The six equivalent Fe–Fe distances in **12S-2** are 2.883 Å (B3LYP) or 2.894 Å (BP86).

3.1.6 $Fe_4C(CO)_{11}$.

Three low-lying $Fe_4C(CO)_{11}$ structures (two singlets and one triplet) were found (Figure 8 and Table 6). All three structures are predicted to have a butterfly skeleton with five Fe–Fe bonds. Both the B3LYP and BP86 methods predict the $Fe_4C(CO)_{11}$ global minimum to be the triplet structure **11T-1**. However, the two DFT methods predict somewhat different geometries. The BP86 method predicts **11T-1** to have C_s symmetry with one semibridging CO group. Structure **11T-1** can be derived from **13S-1** by removing a CO group from each of the butterfly body Fe atoms. The B3LYP method predicts **11T-1** to have C_1 symmetry with all terminal CO groups.

Table 6. The carbon-iron bond distances and the iron-iron bond distances for the three $Fe_4C(CO)_{11}$ structures obtained by the B3LYP and BP86 methoda.

	B3LYP			BP86		
	11T-1	**11S-1**	**11S-2**	**11T-1**	**11S-1**	**11S-2**
C_1-Fe_1	1.804	1.795	1.830	1.820	1.867	1.847
C_1-Fe_2	1.819	1.835	1.830	1.820	1.818	1.847
C_1-Fe_3	1.895	1.954	1.876	1.933	1.937	1.842
C_1-Fe_4	1.996	1.886	1.979	1.914	1.840	1.946
Fe_1-Fe_3	2.658	2.592	2.591	2.627	2.687	2.554
Fe_1-Fe_4	2.597	2.573	2.611	2.573	2.502	2.603
Fe_2-Fe_3	2.583	2.616	2.591	2.627	2.619	2.554
Fe_2-Fe_4	2.620	2.547	2.611	2.573	2.577	2.603
Fe_3-Fe_4	2.659	2.643	2.590	2.503	2.495	2.530

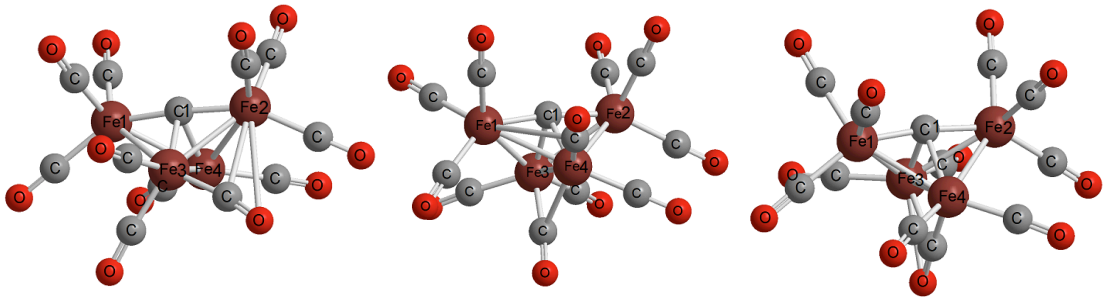

11T-1 (C_s/C_1, 0.0, 0.0) **11S-1** (C_1, 20.2, 1.4) **11S-2** (C_s, 21.4, 1.4)

Figure 8. Three optimized $Fe_4C(CO)_{11}$ structures.

The C_s singlet singly bridged $Fe_4C(CO)_{11}$ structure **11S-2** lies 21.4 kcal/mol (B3LYP) or 1.4 kcal/mol (BP86) kcal/mol in energy above **11T-1** (Figure 8). Structure

11S-2 has a similar geometry to **11T-1** and thus likewise can be derived from **13S-1** by removing a CO group from each of the butterfly body Fe atoms. Structure **11S-2** has a small imaginary vibrational frequency of 28i cm^{-1} (B3lYP) or 16i cm^{-1} (BP86). Following the corresponding normal mode leads to the C_1 structure **11S-1**, with only a slightly lower energy, namely 20.2 kcal/mol (B3LYP) or 1.4 kcal/mol (BP86) relative to **11T-1**. The large difference in the singlet-triplet splittings for $Fe_4C(CO)_{11}$ predicted by the two DFT methods is not surprising, since Reiher and co-workers have concluded that the B3LYP method always favors the higher spin state and the BP86 method favors the lower spin state, with the true energy difference lying between the two values.[39,40]

3.2. Thermochemistry

Table 7 reports the dissociation energies for removing one CO group from the global minima of $Fe_4C(CO)_n$ (n = 16 to 12) structures according to the following equations:

$$Fe_4C(CO)_n \rightarrow Fe_4C(CO)_{n-1} + CO \quad (n = 16 \text{ to } 12).$$

The CO dissociation energies of $Fe_4C(CO)_n$ (n = 16, 15, 14) are all predicted to be less than 12 kcal/mol. However, the CO dissociation energy of $Fe_4C(CO)_{13}$ is much higher, namely, 20.5 kcal/mol (B3LYP) or 26.1 kcal/mol (BP86), suggesting that $Fe_4C(CO)_{13}$ is favored with respect to carbonyl dissociation. This agrees with experiment, since only $Fe_4C(CO)_{13}$ has been synthesized.[5] The carbonyl dissociation energy of $Fe_4C(CO)_{12}$ is even higher, i.e., 24.5 kcal/mol (B3LYP) or 43.7 kcal/mol (BP86) so that $Fe_4C(CO)_{12}$ could be another synthesis target. These CO dissociation energies can be compared with the experimental CO dissociation energies of 27 kcal/mol, 41 kcal/mol, and 37 kcal/mol for $Ni(CO)_4$, $Fe(CO)_5$, and $Cr(CO)_6$, respectively.[41]

Table 7. Bond dissociation energies after zero-point energy corrections (kcal/mol) for successive removal of carbonyl groups from the lowest energy optimized $Fe_4C(CO)_n$ (n = 16 to 12) structures.

	B3LYP	BP86
$Fe_4C(CO)_{16}$ (**16S-1**) → $Fe_4C(CO)_{15}$ (**15S-1**) + CO	1.8	-0.3
$Fe_4C(CO)_{15}$ (**15S-1**) → $Fe_4C(CO)_{14}$ (**14S-1**) + CO	5.8	11.1
$Fe_4C(CO)_{14}$ (**14S-1**) → $Fe_4C(CO)_{13}$ (**13S-1**) + CO	–1.3	6.1
$Fe_4C(CO)_{13}$ (**13S-1**) → $Fe_4C(CO)_{12}$ (**12S-1**) + CO	20.5	26.1
$Fe_4C(CO)_{12}$ (**12S-1**) → $Fe_4C(CO)_{11}$ (**11T-1**) + CO	24.5	43.7

Table 8 reports the energies for the following disproportionation reactions:

$2\ Fe_4C(CO)_n \rightarrow Fe_4C(CO)_{n+1} + Fe_4C(CO)_{n-1}$ (n = 15 to 12)

The disproportionation of $Fe_4C(CO)_{14}$ into $Fe_4C(CO)_{15}$ + $Fe_4C(CO)_{13}$ is an exothermic process by 7.1 kcal/mol (B3LYP) or 5.0 kcal/mol (BP86), suggesting that $Fe_4C(CO)_{14}$ is not a viable species. In contrast, the energy required for disproportionation of $Fe_4C(CO)_{13}$ into $Fe_4C(CO)_{14}$ + $Fe_4C(CO)_{12}$ is 21.9 kcal/mol (B3LYP) or 20.0 kcal/mol (BP86). This is consistent with the synthesis of $Fe_4C(CO)_{13}$ as a stable molecule.[5] The disproportionation energies of $Fe_4C(CO)_{15}$ and $Fe_4C(CO)_{12}$ are 3.9 and 4.0 kcal/mol (B3LYP) or 11.4 and 17.6 kcal/mol (BP86), respectively, suggesting that these species are likely to have limited viabilities.

Table 8. Disproportionation energies after zero point energy correctioins (kcal/mol) for $2Fe_4C(CO)_n \rightarrow Fe_4C(CO)_{n+1} + Fe_4C(CO)_{n-1}$ (n = 15 to 12) processes with the lowest energy structures.

	B3LYP	BP86
$2Fe_4C(CO)_{15}$ (**15S-1**) → $Fe_4C(CO)_{16}$ (**16S-1**) + $Fe_4C(CO)_{14}$ (**14S-1**)	3.9	11.4
$2Fe_4C(CO)_{14}$ (**14S-1**) → $Fe_4C(CO)_{15}$ (**15S-1**) + $Fe_4C(CO)_{13}$ (**13S-1**)	–7.1	–5.0
$2Fe_4C(CO)_{13}$ (**13S-1**) → $Fe_4C(CO)_{14}$ (**14S-1**) + $Fe_4C(CO)_{12}$ (**12S-1**)	21.9	20.0
$2Fe_4C(CO)_{12}$ (**12S-1**) → $Fe_4C(CO)_{13}$ (**13S-1**) + $Fe_4C(CO)_{11}$ (**11T-1**)	4.0	17.6

4. Conclusions

Simple electron counting in $Fe_4C(CO)_n$ clusters requires $n + f$ to be 18 for each iron atom to have the favored 18 electron configuration where n is the number of CO groups and f is the number of Fe–Fe single bonds. This is consistent with a spiropentane structure with two Fe–Fe bonds for the lowest energy $Fe_4C(CO)_{16}$ structure **16S-1** and a butterfly structure with five Fe–Fe bonds for the experimentally known[5] $Fe_4C(CO)_{13}$ structure **13S-1**. Similar considerations suggest a structure with three Fe–Fe single bonds for the pentadecacarbonyl $Fe_4C(CO)_{15}$, which could correspond to a trigonal pyramidal arrangement of the four iron atoms with an apex iron atom forming Fe–Fe single bonds to each of the three basal iron atoms. However, the two lowest energy $Fe_4C(CO)_{15}$ structures **15S-1** and **15S-2** instead have a bent chain of the four iron atoms, also with three Fe–Fe bonds rather than the trigonal pyramidal iron atom arrangement. The lowest energy $Fe_4C(CO)_{14}$ structure **14S-1** has a central Fe_4 trigonal pyramid that is distorted to bring two of the basal iron atoms together to form a fourth Fe–Fe bond in accord with the $n + f$ = 18 rule above to give each iron atom the favored 18-electron configuration.

The maximum number of Fe–Fe bonds in a tetranuclear iron complex is six, corresponding to a tetrahedron. Such an Fe_4C tetrahedron is found in the beautiful but higher energy $Fe_4C(CO)_{12}$ structure **12S-2**, which thus obeys the $n + f = 18$ rule and has ideal T_d tetrahedral symmetry. However, the lowest energy $Fe_4C(CO)_n$ (n = 12, 11) structures are derived from **13S-1** by losses of various CO groups with retention of the central Fe_4C butterfly. No clear indications for Fe-Fe multiple bonding are found in these unsaturated $Fe_4C(CO)_n$ (n = 12, 11) systems. Since the maximum number of Fe–Fe single bonds in an Fe_4 cluster is six, one or more iron atoms in these structures necessarily must have electronic configurations less than the favored 18-electron configuration.

The thermochemical predictions are consistent with the experimental observation that $Fe_4C(CO)_{13}$ is the stable product obtained in the synthesis of tetranuclear iron carbonyl carbides. Thus the CO dissociation energies of $Fe_4C(CO)_n$ (n = 16, 15, 14) are all predicted to be less than 12 kcal/mol (Table 7) whereas the CO dissociation of $Fe_4C(CO)_{13}$ is predicted to be ~23 kcal/mol.

Acknowledgement

This work was partly supported by Special-funded Program on National Key Scientific Instruments and Equipment Development (2012YQ17000408), National Natural Science Foundation of China (61378035), Science and Technology Major Project of Zhejiang Province (2012C12017-5), and 151 Talent Project of Zhejiang Province (12-2-008). We are also indebted to the U. S. National Science Foundation (Grants CHE-1057466, CHE-1054286, and CHE-1361178) for support of this work.

Supporting Information.

Tables S1 to S22: Theoretical Cartesian coordinates for the structures of $Fe_4C(CO)_n$ (n = 16 to 11) using the B3LYP/DZP and BP86/DZP methods; Tables S23 to S44: Theoretical harmonic vibrational frequencies for the structures of $Fe_4C(CO)_n$ (n = 16 to 11) using the B3LYP/DZP and BP86/DZP methods; Tables S45 to S50: Zero point energies (E, in hartrees), relative energies (ΔE, in kcal/mol), and numbers of imaginary vibrational frequencies (Nimag) for the optimized $Fe_4C(CO)_n$ (n = 16 to 11) structures using the B3LYP/DZP and BP86/DZP methods.; Figures 1 to 6: Optimized $Fe_4C(CO)_n$ (n = 16 to 11) structures; Complete Gaussian03 reference (reference 37).

Literature References

(1) Braye, E. H.; Dahl, L. F.; Hübel, W.; Wampler, D. L. *J. Am. Chem. Soc.* **1962**, *84*, 4633.
(2) Churchill, M. R.; Wormald, J.; Knight, J.; Mays, M. J. *J. Am. Chem. Soc.* **1971**, *93*, 3073.
(3) Stewart, R. P.; Anders, U.; Graham, W. A. G. *J. Organometal. Chem.* **1971**, *32*, C49.
(4) Bradley, J. S.; Ansell, G. B.; Hill, E. W. *J. Am. Chem. Soc.* **1979**, *101*, 7417.
(5) Bradley, J. S.; Ansell, G. B.; Leonowicz, M. E.; Hill, E. W. *J. Am. Chem. Soc.* **1981**, *103*, 4968.
(6) Ferrer, M.; Rena, R.; Rossell, O.; Seco, M. *Coord. Chem. Revs.* **1999**, *193–195*, 619.
(7) Reina, R.; Riba, O.; Rossell, O.; Seco, M.; Font-Bardia, M.; Solans, X. *Organometallics* **2002**, *21*, 5307.
(8) Yempally, V.; Zhu, L.; Captain, B. *J. Cluster Sci.* **2009**, *20*, 695.
(9) Sosinsky, B. A.; Norem, N.; Shelly, J. *Inorg. Chem.***1982**, *21*, 348.
(10) Wijeyesekera, S. D.; Hoffmann, R.; Wilker, C. N. Organometallics **1984**, *3*, 972.
(11) Harris, S.; Bradley, J. S. Organometallics **1984**, *3*, 1086.
(12) Stanghellini, P. L.; Sailor, M. J.; Kuznesof, P.; Whiemire, K. H.; Hriljac, J. A.; Kolis, J.W.; Zheng, Y.; Shriver, D. F. *Inorg. Chem.* **1987**, *26*, 2950.
(13) Shriver, D. F.; Sailor, M. J. *Acc. Chem. Res.* **1988**, *21*, 374.
(14) Wade, K., *Chem. Comm.* **1971,** 792.
(15) Wade, K. *Adv. Inorg. Chem. Radiochem*. **1976**, *18*, 1.
(16) Mingos, D. M. P. *Nature Phys. Sci*. **1972**, *99*, 236.
(17) Mingos, D. M. P. *Accts. Chem. Res*. **1984**, *17*, 311.
(18) Anema, S. G.; Barris, G. C.; MacKay, K. M.; Nicholson, B. K. *J. Organometal. Chem.* **1988**, *350*, 207.
(19) Whitmire, K. H.; Lagrone, C. B.; Churchill, M. R.; Fettinger, J. C.; Robinson, B. H. *Inorg. Chem.* **1987**, *26*, 3491.
(20) Ziegler T.; Autschbach, J. *Chem. Rev.* **2005**, *105*, 2695.
(21) Bühl, M.; Kabrede, H. *J. Chem. Theory Comput.* **2006**, *2*, 1282.
(22) Brynda, M.; Gagliardi, L.; Widmark, P. O.; Power, P. P.; Roos, B. O. *Angew. Chem. Int. Ed.* **2006**, *45*, 3804.
(23) Sieffert, N.; Bühl, M. *J. Am. Chem. Soc.* **2010**, *132*, 8056.
(24) Schyman, P.; Lai, W.; Chen, H.; Wang, Y.; Shaik, S. *J. Am. Chem. Soc.* **2011**, *133*, 7977.
(25) Adams, R. D.; Pearl, W. C.; Wong, Y. O.; Zhang, Q.; Hall, M. B.; Walensky, J. R. *J. Am. Chem. Soc.* **2011**, *133*, 12994–12997.

(26) Lonsdale, R.; Olah, J.; Mulholland, A. J.; Harvey, J. N. *J. Am. Chem. Soc*. **2011**, *133*, 15464–15474.
(27) Becke, A. D. *J. Chem. Phys*. **1993**, *98*, 5648.
(28) Lee, C.; Yang, W.; Parr, R. G. *Phys. Rev*. *B* **1988**, *37*, 785.
(29) Becke, A. D. *Phys. Rev. A* **1988**, *38*, 3098.
(30) Perdew, J. P. *Phys. Rev. B* **1986**, *33*, 8822.
(31) Feng, X.; Gu, J.; Xie, Y.; King, R. B.; Schaefer, H. F. *J. Chem. Theor. Comput.* **2007**, *3*, 1580.
(32) Zhao, S.; Wang, W.; Li, Z.; Liu, Z. P.; Fan, K.; Xie, Y.; Schaefer, H. F. *J. Chem. Phys.* **2006**, *124*, 184102.
(33) Dunning, T. H. *J. Chem. Phys*. **1970**, *53*, 2823.
(34) Huzinaga, S. *J. Chem. Phys*. **1965**, *42*, 1293.
(35) Wachters, A. J. H. *J. Chem. Phys*. **1970**, *52*, 1033.
(36) Hood, D. M.; Pitzer, R. M.; Schaefer, H. F. *J. Chem. Phys*. **1979**, *71*, 705.
(37) Frisch, M. J. *et. al*., Gaussian 03, Revision C 02; Gaussian, Inc.; Wallingford CT, **2004** (see Supporting Information for details).
(38) Xie, Y.; King, R. B.; Schaefer, H. F. *Spectrochem. Acta A* **2005**, *61,* 1693.
(39) Reiher, M.; Salomon, O.; Hess, B. A. *Theor. Chem. Acc*. **2001**, *107*, 48.
(40) Salomon, O.; Reiher, M.; Hess, B. A. *J. Chem. Phys*. **2002**, *117*, 4729.
(41) Sunderlin, L. S.; Wang, D.; Squires, R. R. *J. Am. Chem. Soc*., **1993,** *115*, 12060.

5/14

Table of Contents Entry

From Spiropentane to Butterfly and Tetrahedral Structures in Tetranuclear Iron Carbonyl Carbide Chemistry

Xiaoli Gong,* Liyao Zhu, Jing Yang, Xiumin Gao, Qian-shu Li, Yaoming Xie, R. Bruce King,* and Henry F. Schaefer III

The geometries of the lowest energy $Fe_4C(CO)_n$ (n = 16, 15, 14, 13) structures obey the $n + f = 18$ rule where f is the number of Fe–Fe bonds. This leads to a spiropentane geometry for $Fe_4C(CO)_{16}$, a central bent Fe–Fe–Fe–Fe chain for $Fe_4C(CO)_{15}$, a distorted trigonal pyramidal structure for $Fe_4C(CO)_{14}$, and the experimentally observed butterfly structure for $Fe_4C(CO)_{13}$. The lowest energy $Fe_4C(CO)_n$ (n = 12, 11) structures are derived from the lowest energy $Fe_4C(CO)_{13}$ by removal of CO groups with retention of the central Fe_4C butterfly unit.

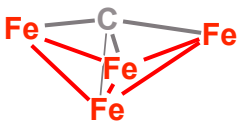

Butterfly
$Fe_4C(CO)_{13}$